

In vitro and in vivo biocompatibility evaluation of a 3D bioprinted gelatin-sodium alginate/rat Schwann-cell scaffold

Zongxi Wu^{a,b,c,d,1}, Qing Li^{b,c,d,e,1}, Shang Xie^{a,b,c,d}, Xiaofeng Shan^{a,b,c,d},
Zhigang Cai^{a,b,c,d,*}

^a Department of Oral and Maxillofacial Surgery, Peking University School and Hospital of Stomatology, Beijing, China

^b National Clinical Research Center for Oral Diseases, Beijing, China

^c National Engineering Laboratory for Digital and Material Technology of Stomatology, Beijing, China

^d Beijing Key Laboratory of Digital Stomatology, Beijing, China

^e Center of Digital Dentistry, Peking University School and Hospital of Stomatology, Beijing, China

ARTICLE INFO

Keywords:

Gelatin
Sodium alginate
3D bioprinting
Schwann cells
Neural tissue engineering

ABSTRACT

Peripheral nerve injuries often cause different degrees of sensory and motor function loss. Currently, the repair effect of the “gold standard”, autologous nerve transplantation, is unsatisfactory. Tissue engineering has the potential to tissue manipulation, regeneration, and growth, but achieving personalization and precision remains a challenge. In this study, we used 3D bioprinting to construct a nerve scaffold composed of gelatin/alginate hydrogel containing rat Schwann cells. On day 1 after printing, the Schwann cell survival rate was $91.87 \pm 0.55\%$. Cells could be cultured in the hydrogel for 7 days, and were well attached to the surface of the scaffold. On days 4 and 7, the 3D bioprinted scaffold released higher levels of nerve growth factor (NGF) than 2D culture group. Further, the mRNA levels of NGF, brain-derived neurotrophic factor (BDNF), glial-derived neurotrophic factor (GDNF), and platelet-derived growth factor (PDGF) expressed on day 4 by Schwann cells were higher in the 3D bioprinted scaffold culture than in 2D culture. After 4 weeks of implantation, the cell-containing scaffold still showed partial lattice structure and positive S-100 β immunofluorescence. These results indicated that the 3D bioprinted gelatin-sodium alginate/Schwann-cell composite scaffold improved cell adhesion and related factor expression. This 3D bioprinted composite scaffold showed good biocompatibility and could be a promising candidate in neural tissue engineering in the future.

1. Introduction

Peripheral nerve injury (PNI) causes different degrees of sensory and motor function loss [1], which affects patients physiologically and psychologically [2]. The incidence of PNI is 12–23 per 100,000 people in the US and Europe [3–5]. Current treatments for peripheral nerve injuries include autologous nerve grafting, motor nerve anastomosis of the defective nerve and other adjacent sites, and vascularized nerve grafting [6]. Autologous nerve grafting has become the gold standard for surgical repair of peripheral nerve defects [7]. However, autologous nerve grafting has several limitations such as nerve torsion or misalignment, limited donors, and loss of donor function, which make the repair effect unsatisfactory [8].

The recent development of nerve conduits containing scaffolds,

cells, and growth factors could address the limitations currently associated with the treatment of PNI and these conduits could emerge as an ideal transplant substitute [9]. Advantages of using a nerve conduit include reducing secondary damage, providing access to guide axons from proximal to distal growth, and reducing the formation of scar tissue that can impede nerve regeneration [10]. Natural and synthetic polymer artificial nerve conduits comprising collagen, gelatin, sodium alginate, silk, polycaprolactone, polyurethane, etc. have been developed for axonal regeneration [11,12]. However, traditional tissue engineering techniques including dip coating, electrospinning, phase separation, self-assembly, molding and sheet rolling [13,14] have the disadvantages of complicated production processes and limited customization and precision, which increase the rate of surgical failure.

3D printing, an emerging tissue engineering scaffolding technology,

* Corresponding author at: Department of Oral and Maxillofacial Surgery, Peking University School & Hospital of Stomatology, 22 Zhongguancun South Avenue, Haidian District, Beijing 100081, China.

E-mail address: c2013xs@163.com (Z. Cai).

¹ These authors contribute equally to this work.

enables spatial control of functional component placement to create complex 3D scaffolds. Computer aided design and adjustment of formulation of printed materials can produce controlled porosity and mechanical properties, while enabling personalized printing and precise three-dimensional structure [15], which increase the likelihood of complete recovery after neurological defects. Xu et al. [16] used fibrin gel to print nerve scaffolds that were used to culture embryonic hippocampus and cortical neurons, and found that the cell survival rate was $74.2 \pm 6.3\%$. Fibrin gel was therefore considered beneficial to neuronal adhesion and promotion, cell migration and proliferation, and matrix synthesis. Wang et al. [17] used 1.5% alginate and 0.75% hyaluronic acid to print nerve scaffolds, and found that alginate with hyaluronic acid was more conducive to Schwann cell adhesion than pure hyaluronic acid, which was not conducive to Schwann cell adhesion. Most studies to date have been limited to a single tubular structure that lacked internal structure, which could be addressed by using computer aided design in 3D printing to build a high-precision, multi-level bionic structure and verify its efficacy.

Alginate is a readily and available natural biopolymer with long-term stability that can be purified to prevent immunogenicity [18]. Rowley et al. [19] showed that protein adsorption was hindered by the high hydrophilicity of alginate, which prevented cells from attaching to the scaffold. This could be addressed by modifying the surface of the alginate with a peptide such as Arg-Gly-Asp (RGD) to provide a molecular binding site for cell adhesion [20]. Gelatin retains the RGD sequence, which is less immunogenic and promotes cell adhesion [21]. Therefore, combining alginate and gelatin facilitates cells adherence to the surface of the scaffold.

When the peripheral nerve is damaged, Schwann cells begin to divide, proliferate, and secrete a variety of neurotrophic factors and extracellular matrices, which can express a series of cell adhesion molecules and receptors; these synergistically promote, guide, and regulate axon growth [22]. In addition, Schwann cells participate in the regeneration of myelin and guide axon growth during nerve regeneration, and are therefore indispensable core cells in nerve regeneration tissue engineering.

Although many researchers have printed various cells in alginate-gelatin hydrogels (Ouyang et al. [23]; Zhao et al. [24]), studies on peripheral nerve injury repair are rare. Studies have used hyaluronic acid and polyvinyl alcohol to increase the viscosity of fibrinogen and thrombin solutions respectively, and successfully produced a nerve scaffold that allows Schwann cells to proliferate and maintain activity [25]. In addition, collagen tube grafts containing BMSC and SC were successfully printed [26]. However, the effect of 3D bioprinted nerve scaffolds containing Schwann cells on peripheral nerve regeneration needs further investigation. In this study, we aimed to create a three-dimensional scaffold loading with Schwann cells precisely by 3D

bioprinting, in order to mimic in-vivo ECM properties and simulate the microenvironment of the living cells in the body, thereby enabling Schwann cells to survive and adhere in scaffold. Additionally, the expression of neuro-related trophic factor and immunological markers in the 3D bioprinted scaffold cultures were determined in vitro and biocompatibility was tested in vivo.

2. Materials and methods

2.1. Cell culture

Rat Schwann cells (one week old, primary cells which can be passed to P5) were purchased from CHI SCIENTIFIC (1-5060) and maintained in Dulbecco's Modified Eagle Medium/F12 (Gibco, Grand Island, NY, USA, 11330-032) supplemented with 10% fetal bovine serum (Gibco, 10099-141) and 1% penicillin/streptomycin (Gibco, 15140-122). The cells were cultured at 37 °C in a humidified atmosphere and the medium was renewed every 2 days. Cells were passaged every 3–4 days.

2.2. Material preparation

Gelatin (Sigma-Aldrich, V900863) and sodium alginate (Sigma-Aldrich, 180947) were sterilized by UV lamp irradiation for 30 min before use. The powder dissolved in DMEM/F12, which is made up of 10% FBS and 1% penicillin-streptomycin, then the 2.2% alginate and 9.1% gelatin solution were obtained. Rat Schwann cells were digested with trypsin and resuspended in culture medium. The cell suspension was then gently mixed with the hydrogel precursor to achieve a final concentration of 2% sodium alginate, 8% gelatin, and 2×10^6 cells/ml.

2.3. Cell proliferation analysis and CaCl_2 concentration/time experiment

Cell Counting Kit-8 (CCK8, Japan, LK815) was used to evaluate cell proliferation on day 1, 3, 5, and 7 after treatment with the leaching solution and CaCl_2 solution. For testing the toxicity of the leaching solution, the initial sample cell counts were all 800, and the control group had no leaching solution. For the CaCl_2 treatment test, the initial sample cell counts were all 800, the test component concentrations were 50 mM, 100 mM, 250 mM, and 500 mM, the experimental time components were 5 min and 10 min, and the control group had no CaCl_2 solution. Briefly, the CCK8 solution was mixed with the medium at a ratio of 1:9 to obtain a working solution, and the sample ($n = 3$) at each time point was incubated with 110 μl of the working solution for 2 h. The supernatant was transferred to a 96-well plate, and the absorbance (OD) value of the plate at a wavelength of 450 nm was measured using a microplate reader (BioTek ELX800, VT, USA).

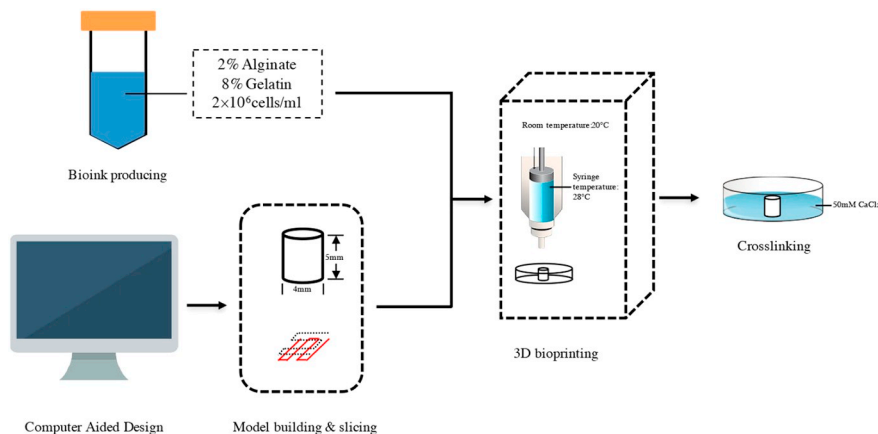


Fig. 1. Schematic illustration for 3D bioprinting.

2.4. 3D bioprinting

The 3D bioprinting procedure is shown in Fig. 1. Briefly, before 3D bioprinting, a cylinder, 5 mm in height and 4 mm in diameter, was pre-designed in the Medprin bioprinter (BMP-C300-T300-IN3) program and the graphics were sliced at a height of 300 μm per layer (Supplementary Fig. 1). The cell-hydrogel mixture was loaded into a 1 ml syringe prior to printing. Considering the biomimetic structure and cell viability, a printing nozzle having an inner diameter of 160 μm was selected. After repeated tests, the room temperature was set at 20 $^{\circ}\text{C}$, and the syringe of the aqueous gel was kept at 28 $^{\circ}\text{C}$. By selecting these parameters, gelatin-alginate could be kept in a liquid state and allowed to gel rapidly on the printing platform during deposition, while the cells maintained high survival rates. The extrusion speed and the nozzle scanning speed were set to 0.15 ml/s and 3.5 mm/s, respectively. After the scaffold was printed, it was immersed in a 50 mM sterilized CaCl_2 solution for 5 min for crosslinking.

2.5. Cell alignment and scaffold morphology

The morphology of the print scaffold was observed using an environmental scanning electron microscopy (ESEM; Quanta 200, FEI, Netherland). After the samples were lyophilized, scaffold morphology and cell adhesion were observed under the saturation pressure of water vapor (1 Torr) and 15 kV accelerating voltage. Multiple areas were randomly selected for photographing.

2.6. Fourier transform infrared spectroscopy (FTIR) analysis

The chemical composition of the scaffold was investigated by Fourier transform infrared spectroscopy (FTIR; Spectrum GX, USA). Using a cell-free scaffold as a control, each sample was ground together with KBr in an agate mortar, at a rate of about 1:20, and compressed into tablets. The spectral range was set from 4000 to 400 cm^{-1} with a resolution of 4 cm^{-1} and a scan time of approximately 100 s.

2.7. Cell viability analysis

A fluorescent live/death viability assay kit (KeyGEN Bio-TECH, China, KGAF001) was used to assess cell viability in the printed scaffold. Briefly, 8 μM propidium iodide (PI) and 2 μM Calcein-AM in PBS were dispensed, after which the printed scaffold was soaked therein. After incubation for 30 min, the scaffold was washed three times with PBS buffer and observed under a fluorescence microscope. Living cells are stained green by Calcein-AM (490 nm), and PI stains dead cells in red (535 nm). For cell viability calculations, the number of live/dead cells was counted in 10 real-time randomly amplified fields per sample ($n = 3$) at $100\times$.

2.8. S100 β immunofluorescence analysis

The 3D bioprinted hydrogel scaffold was subjected to S-100 β immunostaining to determine the expression of characteristic proteins of rat Schwann cells. Briefly, on days 4 and 7 of culture, the scaffold was recrosslinked with 50 mM calcium chloride solution for 5 min and fixed with 4% paraformaldehyde for 30 min. The scaffold was then closed with a blocking solution (Beyotime, China, P0260) for 30 min. Rabbit anti-rat S100 β antibody (Abcam, ab52642) was diluted (1:100) in antibody dilution buffer (Beyotime, China, P0262). Thereafter, the scaffold was immersed in a rabbit anti-rat S100 β antibody solution at 4 $^{\circ}\text{C}$ overnight. On the next day, the residual liquid was aspirated and the scaffolds were gently rinsed three times with PBS. The secondary goat anti-rabbit antibody (Abcam, ab150077) was diluted with a secondary antibody dilution buffer (Beyotime, China, P0265) to 1:500. The samples were incubated with the secondary antibody solution for 1 h. After rinsing three times with PBS, samples were stained with DAPI staining

solution (ZSGB-BIO, ZLI-9557) for 10 min, and viewed under a fluorescence microscope.

2.9. NGF release analysis

Rat nerve growth factor (NGF) ELISA (RayBio, USA, 121418 0719) was used to quantitatively determine the release of NGF in the 2D culture and 3D bioprinted groups. Briefly, the initial cell number and the medium volume of the 2D and 3D cultures were adjusted to be the same. On days 4 and 7, the cell culture supernatant was collected and centrifuged at 1000 rpm for 10 min. Samples and standards were then incubated in 96-well ELISA plates coated with anti-NGF antibodies. After 2.5 h, biotin antibody and streptavidin solution were added in sequence, and incubated for 1 h and 45 min, respectively. The TMB substrate was then added for 30 min to develop the color, and the reaction was stopped using stop solution. The OD value was immediately read at a wavelength of 450 nm on a microplate reader.

2.10. Quantitative real-time polymerase chain reaction (qRT-PCR)

Gene expression ($n = 3$) of cells cultured on the 3D bioprinted scaffold for 7 days was analyzed. The scaffold was soaked in 50 mM sodium citrate for 10 min and gently stirred to depolymerize the hydrogel. After decrosslinking, the decapsulated cells were centrifuged at 10,000 RPM for 10 min and the pellet was washed with PBS and centrifuged again at 10,000 RPM for 3 min. Total RNA was then extracted using RNeasy Micro Kit (Qiagen, Austin, TX, US) according to the manufacturer's protocol. PrimeScriptTM RT Reagent Kit (TaKaRa, Japan) was used for reverse transcription. FastStart Universal SYBR Green Master (Rox) (Roche, Germany, 04913850001) was used for Quantitative Real-time PCR. Primers for nerve growth factor (NGF), brain-derived neurotrophic factor (BDNF), glial-derived neurotrophic factor (GDNF), and platelet-derived growth factor (PDGF) were synthesized by Sangon Biotech (Table 1). GAPDH was used as a cycle threshold (Ct value), and the fold difference was calculated by the Ct method ($2^{-\Delta\Delta\text{Ct}}$ method).

2.11. In vivo experiments

In order to verify the biocompatibility of the 3D bioprinted constructs containing cells in vivo, the 3D bioprinted constructs were placed subcutaneously of nude mice for in vivo experiments. Animal experiments were performed in accordance with the ethical principles of the Peking University Institutional Animal Care and Use Committee. (License No. LA2018216). The implants were divided into two groups: 3D bioprinted construct containing no Schwann cells, and 3D bioprinted construct containing Schwann cells. On day 1 after printing, 7-week-old male BALB/c nude mice (Vitalriver, weight 20 ± 1 g) were randomly divided into two groups and anesthetized with 4% chloral hydrate. The implants were placed aseptically in the subcutaneous area of the back and labeled accordingly ($n = 6$). All animals were

Table 1
Primer sequences used to amplify the targeted genes.

Genes	Primes
NGF	F: CAACAGGACTCACAGGAGCAAGC R: GATGTCGGTGGCTGTGGTCTTATC
BDNF	F: TGGAAGCTCGCAATGCCGAAGTAC R: TCCTTATGAACCGCCAGCCAATTC
GDNF	F: AAGGTCCGACAGGCCAGAGG R: CCGCTTACAGGAACCGCTAC
PDGF	F: TGTAACACCAGCAGCGTCAAGTG R: CACCTCACATCCGTCTCTCTCTC
GAPDH	F: TCAACGGCACAGTCAAGG R: TGAGCCTTCCACGATG

maintained at 20–25 °C under a 12-hour light/dark cycle. Four weeks after surgery, nude mice were sacrificed by cervical dislocation and the implants were harvested. The implants were fixed in 4% formalin fixative, dehydrated, and embedded in paraffin. The sections were performed using a rotary microtome with a thickness of 4–6 μm . HE staining: Before dyeing, the paraffin in the sections should be removed with xylene, and then immersed in distilled water through a high concentration to a low concentration of alcohol. Then, the sections were soaked in the hematoxylin dye solution for 5–15 min, washed with tap water, differentiated with hydrochloric acid alcohol, and rinsed with running water. It was further soaked in eosin alcohol for 3–5 min, dehydrated with pure alcohol, then made transparent with xylene, and finally sealed with neutral gum. Schwann cells were assessed by immunohistochemistry (IHC) for S-100 β .

2.12. Statistical analysis

Data were expressed as mean \pm standard deviation and analyzed using the SPSS 20.0 software. The *t*-test was used to confirm the homogeneity of variance, and one-way analysis of variance and LSD test were performed. The significance level was $\alpha = 0.05$. $p < 0.05$ was considered a statistically significant difference.

3. Results

3.1. Material biocompatibility and printability

The leaching solution of 2% sodium alginate and 8% gelatin had no significant effect on the proliferation of Schwann cells on days 1, 3, 5, and 7 (Fig. 2a), indicating that Schwann cells had good compatibility with the hydrogel, which showed no cytotoxicity. Schwann cells were treated with CaCl_2 at concentrations of 50 mM, 100 mM, 200 mM, and 500 mM for 5 and 10 min, respectively (Fig. 2b–c). 50 mM CaCl_2 treatment for 5 min showed minimal effects on Schwann cell proliferation. Thus, the crosslinker concentration and time were determined as 50 mM and 5 min, respectively for this experiment. The biomaterial was fitted for 3D bioprinting: the 3D bioprinted constructs maintained their original geometric shape, the edges were clear, and no lines were stuck (Fig. 2d–e). Although the material collapsed partly, the diameter and height of the printed product could still be maintained at both 4.5 mm. When the scaffold was immersed in the medium, there was some degree of expansion, but the original geometry remained intact after 7 days.

3.2. Environmental scanning electron microscopy (ESEM)

Fig. 3a shows the surface of a printed scaffold observed using environmental scanning electron microscopy. The surface of the nerve scaffold was rough, with a large number of pores and adhered Schwann cells. Magnification showed that the Schwann cell elongated (indicated by the arrow) and attached well to the scaffold (Fig. 3b).

3.3. FTIR analysis

As shown in Fig. 4, 3394 cm^{-1} is the sodium alginate hydroxyl bond (OH), 2935 cm^{-1} is the CH_2 group stretching vibration, and 1660 cm^{-1} is the C = O group of amide I stretching and vibration. 1543 cm^{-1} is the NH group bending vibration of amide II, 1410 cm^{-1} is the sodium alginate symmetry-COO stretching (COOH group), and 1238 cm^{-1} is the NH group of amide III of gelatin. 1031 cm^{-1} was an anti-symmetric stretch of COC from sodium alginate. Both groups showed patterns consistent with the peaks of the gelatin and sodium alginate spectra, but the transmittance was different, and the cell-containing transmittance was lower than that of the cells-free scaffold.

3.4. Live/dead cell staining

The live/dead cell ratio was determined using Calcein-AM/PI to analyze the viability of Schwann cells in the 3D bioprinted construct (Fig. 5) within 7 days of culture. Calcein-AM bound live cell membranes appeared green and PI stained dead cell nuclei red. Most of the cells in all groups were stained green, indicating good viability. As observed in the fluorescence images taken on day 1, dead cells were evenly distributed in the scaffold (Fig. 5b). We counted the number of living cells and dead cells to obtain cell viability; the survival rate of the cells was $91.87 \pm 0.55\%$ on day 1, $92.83 \pm 0.46\%$ on day 4, and $93.20 \pm 0.52\%$ on day 7 (Fig. 5j), and there was statistical significance between day 1 and day 7 ($p < 0.01$).

3.5. S100 β immunofluorescence

S100 β is a typical Schwann cell cytoplasmic marker protein involved in growth, cell signaling, movement and functional protein expression. Immunofluorescence staining using S100 β antibody was performed in the printed constructs on days 4 and 7 after printing. As shown in Fig. 6, most cells expressed S100 β , indicating that the printing process and 3D culture did not inhibit S100 β expression.

3.6. Nerve growth factor secretion

The release of NGF from 3D bioprinted scaffold and 2D cultured was evaluated using an ELISA kit. Tests were performed by collecting cell culture medium on days 4 and 7 after printing. The final result was normalized to the concentration of NGF (pg/ml) released per million cells. Fig. 7 shows that, under 2D culture, the NGF release on days 4 and 7 were 15.71 ± 0.09 and 27.35 ± 2.18 pg/ml, respectively. On days 4 and 7, the NGF release in 3D bioprinted cells were 24.86 ± 1.21 and 38.71 ± 5.34 pg/ml, respectively. On days 4 and 7, there was a statistically significant difference between the 3D and 2D culture results, and the levels of NGF released from 3D bioprinted cells was significantly higher than those from 2D cultures.

3.7. Nerve-regeneration-related gene expression

Nerve-regeneration-related gene expression can reflect differences in neuronal function. Gene expression levels of NGF, BDNF, GDNF, and PDGF in the 3D and 2D groups were measured on day 4. The mRNA expression of the four genes was higher in the 3D group than in the 2D group ($p < 0.05$; Fig. 8).

3.8. In vivo experiments

After 4 weeks of implantation, the 3D bioprinted scaffolds were harvested (Fig. 9a–c). Scaffolds without Schwann cells were degraded. Scaffolds with Schwann cells were loose in structure, and the volume was smaller than that before implantation. The texture was soft and brittle, and it was difficult to clamp. HE staining (Fig. 9d–e) showed that few inflammatory response or immune rejection, and part of the scaffold grid was retained in the cell group. Immunofluorescence showed positive S-100 β staining (Fig. 9f).

4. Discussion

Alginate and gelatin have been widely used in 3D printing as encapsulating materials for various cell types, including hematopoietic cell lines (U937) and fibroblasts [27], human endothelial cells [28], osteoblast-like cells (MG-63), and chondrocytes [29] in several studies, where they enhanced cell proliferation and functional expression. We treated Schwann cells with leaching solution, which did not affect cell proliferation, indicating that the material has good biocompatibility with Schwann cells. Sodium alginate encounters calcium ions and

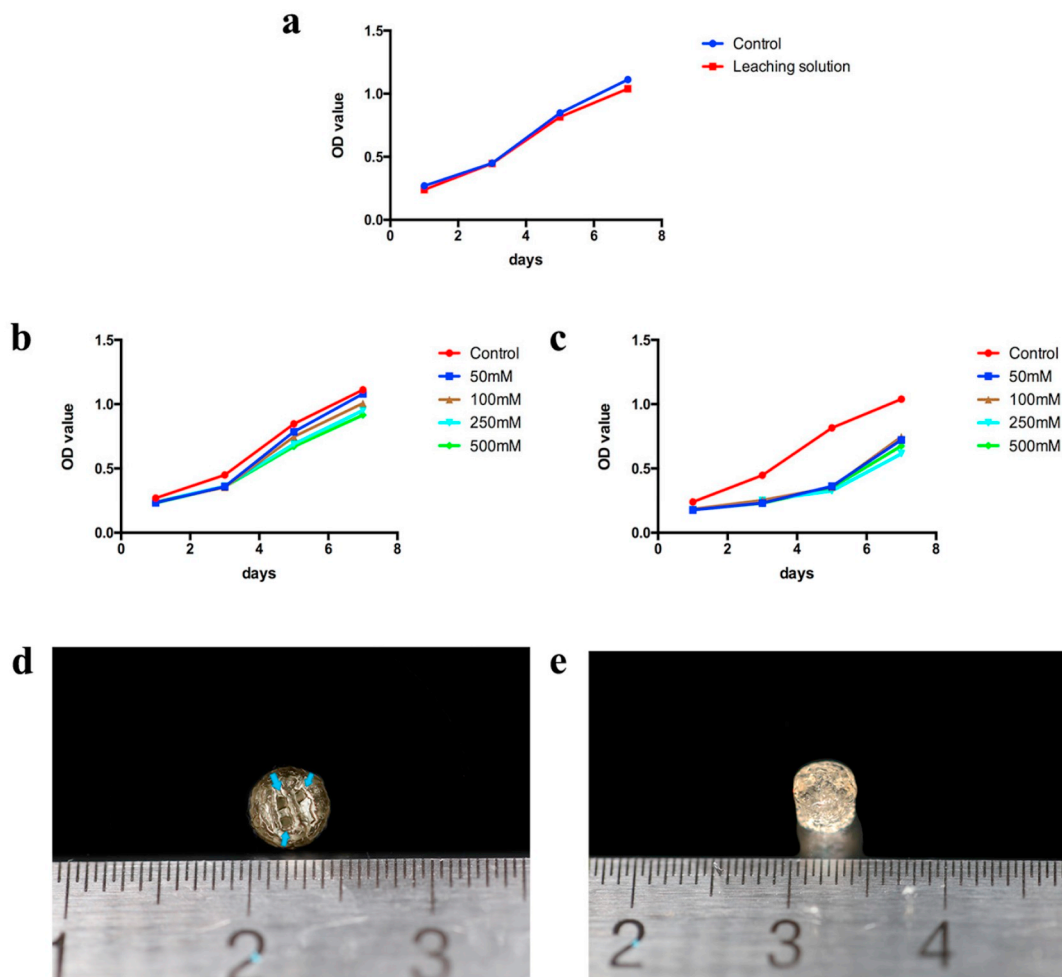


Fig. 2. Material biocompatibility and printability: a) Leaching solution treated Schwann cells test by CCK8, b) CaCl₂ treated Schwann cells for 5 minute test by CCK8, c) CaCl₂ treated Schwann cells for 10 minute test by CCK8, d) Vertical view of 3D bioprinting of Gelatin/Sodium Alginate scaffold, the arrows indicate the void channel inside the scaffold, e) Front view of 3D bioprinting of Gelatin/Sodium Alginate scaffold.

undergoes rapid ion exchange to form a gel [30]. Sarker et al. [31] showed that even 20 consecutive layers of Ca²⁺ ion-crosslinked alginate chains formed square pores, while Ba²⁺ and Zn²⁺ ion-crosslinked alginate chains produced imperfect square pores. Thus, the printable concentration of the Ca²⁺ ion crosslinker is typically maintained at 50–150 mM. In this study, treatment with 50 mM CaCl₂ for 5 min had the least effect on Schwann cells. Although only 5 min of cross-linking caused a certain degree of swelling in the scaffold for 7 days, the scaffold maintained its entire shape without falling apart.

Compared with 2D culture, 3D bioprinting could provide more

space and a better microenvironment for cell proliferation and expression of functional proteins to mimic the three-dimensional growth of cells in vivo. In this study, we used gelatin and sodium alginate hydrogel loaded with Schwann cells for 3D bioprinting, and evaluated cell viability, immunofluorescence, related protein secretion, and mRNA content in vitro, and placed the scaffold in vivo to observe its function.

The percentage of gelatin and sodium alginate affects the printability of the hydrogel. Duan et al. [32] used 6% gelatin and 8% sodium alginate to print aortic root sinus smooth muscle cells and aortic valve

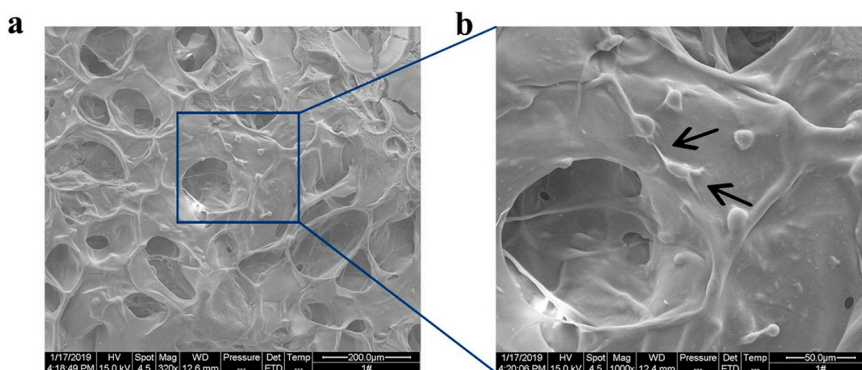


Fig. 3. Scaffold morphology by ESEM analysis: Gelatin/Sodium Alginate scaffold at 320× (a) and 1000× (b), the arrows indicate pseudopod from Schwann cell.

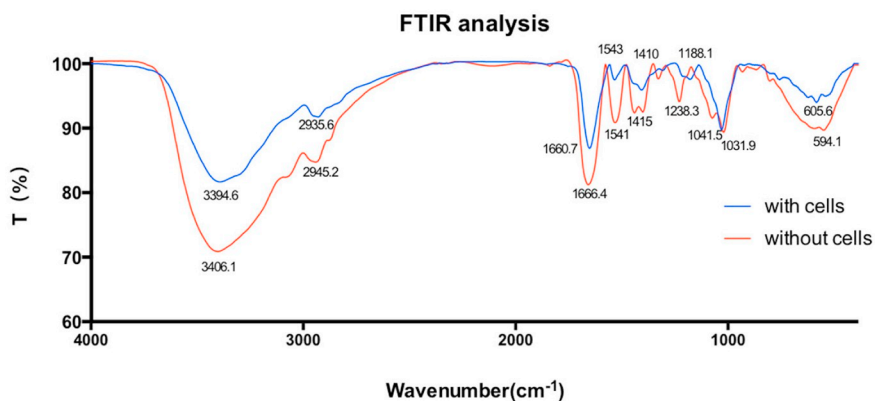


Fig. 4. FTIR of gelatin-sodium alginate hydrogels with/without Schwann cells.

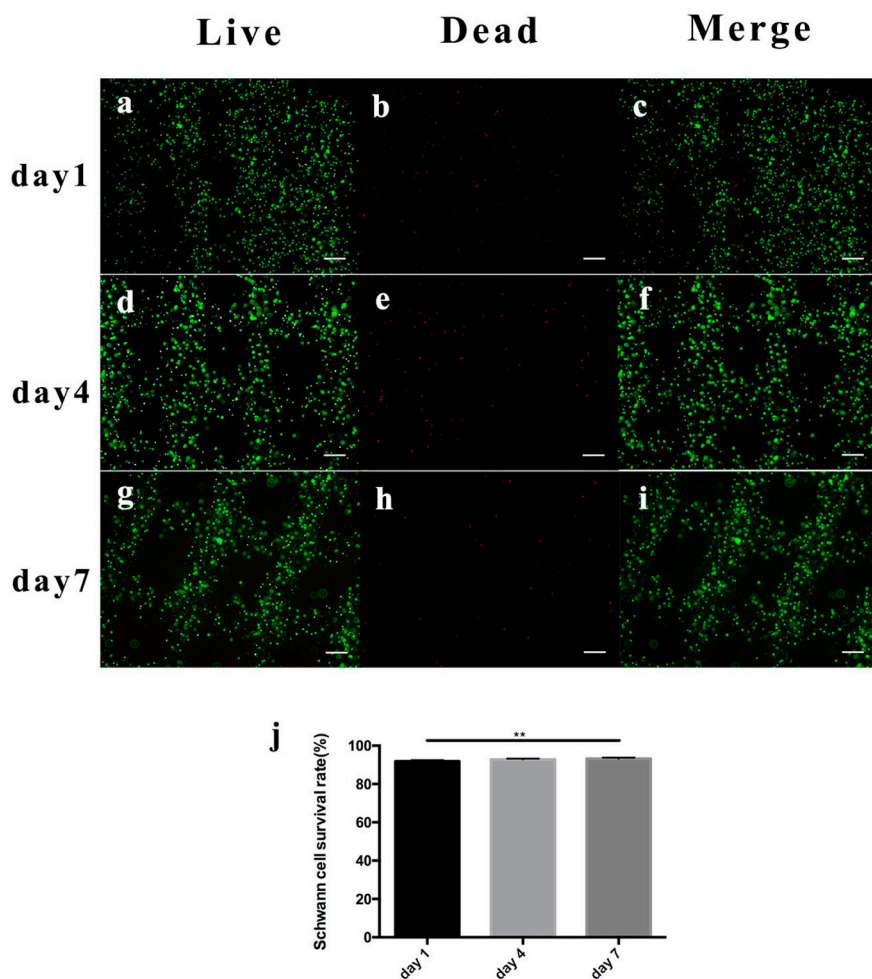


Fig. 5. Live/dead cell staining: a–i. Live cells (a, d, g), dead cells (b, e, h), and merge images (c, f, i) on days 1, 4, and 7 after 3D bioprinting. (Scale bar: 100 μm), j cell viability results on days 1, 4, and 7. (** $p < 0.01$).

leaflet interstitial cells, while Giuseppe et al. [33] proposed that 7% sodium alginate and 8% gelatin could produce high printability. In this study, the biological scaffold maintained a certain geometry and height after 3D bioprinting, indicating that the hydrogel mixed with 2% sodium alginate and 8% gelatin could be extruded at 28 $^{\circ}\text{C}$ to form a gel with good plasticity. In addition, we used a needle diameter of 160 μm , which is smaller than most printing nozzles (250–450 μm) [34], but considerably larger than axons (0.2–16 μm) [35].

Lin et al. [36] demonstrated that the electrostatically bound gelatin to alginate fibers and modified the surface of macropores to provide cell

adhesion molecules that facilitate nerve cell attachment and growth. As shown in the Fig. 2, Schwann cells were embedded in the 3D bioprinted scaffold, which enhanced its function. Further, the Schwann cells elongated on the scaffold surface and were well connected to each other, indicating good cell-scaffold compatibility, which would improve cell proliferation and function.

Lopes et al. [37] showed a peak of the dehydrated alginate/gelatin microcapsules with a hydrogen-linked functional group O–H at 3454 cm^{-1} , and the peak observed at 2185 cm^{-1} was attributed to the CO_2 group. An increase in the intensity of the CONH_2 (C=O) peak

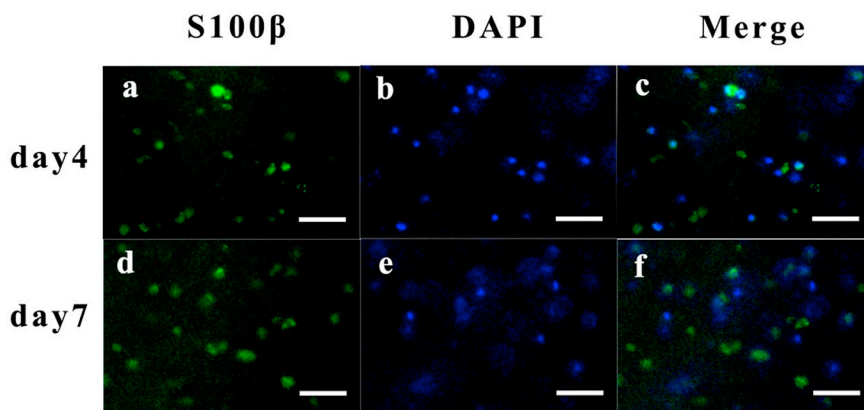


Fig. 6. Immunostaining of S100β marker on day 4 and 7: S100β staining (a, d); DAPI staining (b, e); merge image (c, f). (Scale bar: 50 μm).

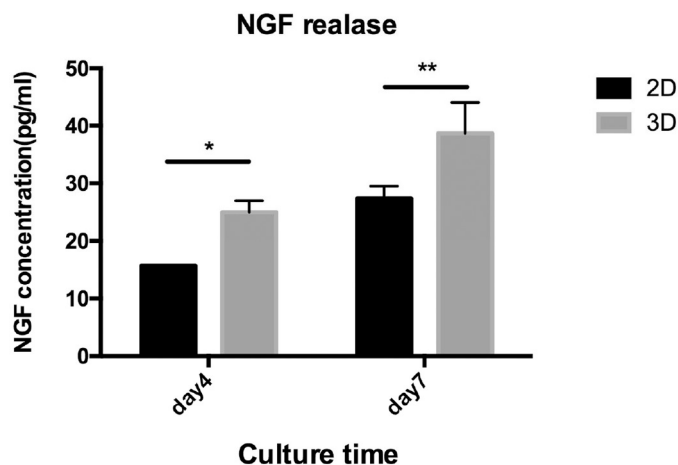


Fig. 7. NGF release (by ELISA) of 3D bioprinted and 2D culture on days 4, 7 (*p < 0.05, **p < 0.01).

corresponding to 1637 cm⁻¹ indicates that the negative group of alginate may be associated with the positive loading of gelatin. This was consistent with the results of this study, showing that 3D bioprinting did not change the original properties of the scaffold components. The peak of the cell-containing group was slightly lower than the peak of

the no-cell group, possibly owing to various cell-related impurities, which affect the absorption of infrared light by the corresponding group, but not the original properties of the scaffold.

High expandability is an advantage of extruded hydrogels, but is associated with a loss of resolution. The resolution can be improved by reducing the nozzle diameter, but increasing the shear force could cause cell damage [38]. Cell viability in scaffolds range from 40% to 95% depending on hydrogel viscosity, cell concentration, and nozzle size [39]. Hydrogel concentration also affects cell survival. A mixture of 5% gelatin and 1% alginate maintained almost 100% viability; however, a mixture of 10% gelatin and 1% alginate, showed a viability of the vitality 70% after 6 h of printing [40]. Further, 2% alginate concentration maintained about 90% viability, while 6% alginate concentration only maintained 35% [41]. In this study, we used a 160 μm diameter nozzle to print. After printing, the survival rates of cells on days 1, 4, and 7 were 91.87% ± 0.55, 92.83% ± 0.46, and 93.20% ± 0.52, respectively, indicating that the cells were slightly affected by shear force during printing, but survived for seven days. Thus, the hydrogel composition of 2% sodium alginate and 8% gelatin was suitable for Schwann cell survival.

The S100β subunit is a cytosolic calcium-binding protein that plays an important role in growth, cell signaling, movement, and metabolism [42]. Soucy et al. [43] used gelatin-methacryloyl (GelMA) and methacryloyl-substituted tropoelastin to culture Schwann cells. Immunofluorescence showed that Schwann cells were round and expressed

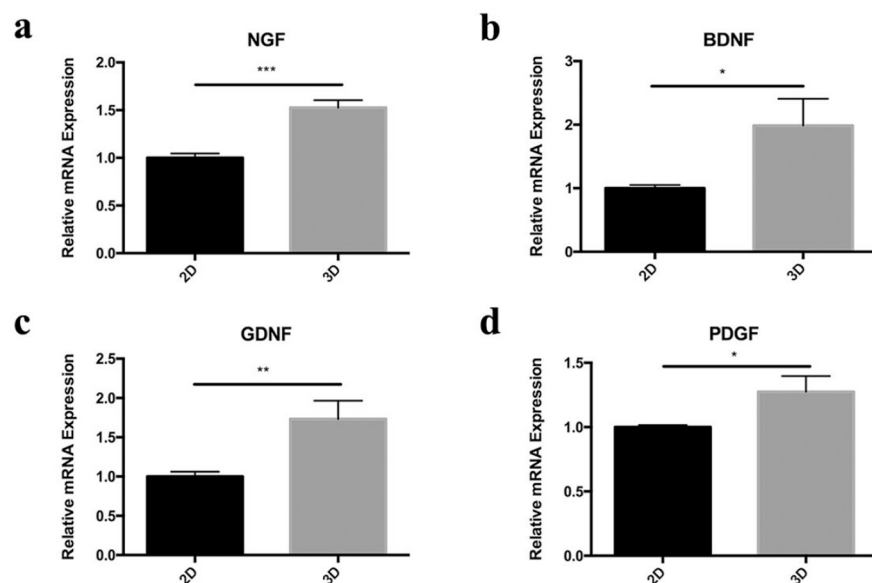


Fig. 8. Quantitative comparison of NGF (a), BDNF (b), GDNF (c) and PDGF (d) gene expression was detected by qRT-PCR on day 4. Compared to 2D culture, the mRNA expression levels of 3D bioprinted group were analyzed by the 2^{-ΔΔCt} method using GAPDH as the internal control. Dates were represented as the mean ± SD (n = 3). (*p < 0.05, **p < 0.01 and ***p < 0.001).

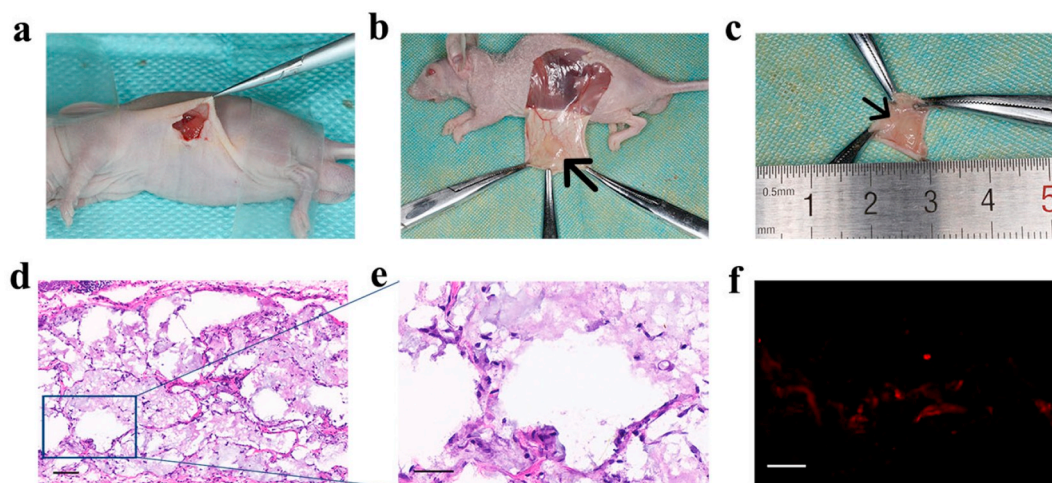


Fig. 9. In vivo experiment: a) The 3D bioprinted scaffold during implantation, b) After 4 weeks implantation, the arrow indicates the 3D bioprinted scaffold, c) The arrow showed the 3D bioprinted scaffolds, d) H&E staining of paraffin embedded sections at 4 weeks after implantation ($8.4\times$, scale bar $100\ \mu\text{m}$), e) Magnification of H&E staining ($26.7\times$, scale bar $50\ \mu\text{m}$), f) S100 β immunohistochemical staining (scale bar $50\ \mu\text{m}$).

S100 β antibody. In this study, gelatin and alginate was used as a composite scaffold material, and immunofluorescence showed that cells with S100 β antibody were expressed in the scaffold, indicating that 3D printing did not affect the phenotype of Schwann cells. Schwann cells showed a round shape on day 4, indicating that Schwann cells were suspended in the hydrogel. On day 7, Schwann cells showed a dendritic shape, indicating that the cells adhered well to the scaffold.

Nerve growth factor (NGF) is a secreted protein that promotes axonal regeneration and improves electrophysiological and histomorphometric parameters after nerve injury [44,45]. Li et al. [46] treated diabetic rats with sciatic nerve injury with NGF-loaded heparin-polyoxamer thermogels, which promoted exercise recovery and Schwann cell proliferation. Chao et al. [47] used a chitosan/glycerophosphate hydrogel loaded with NGF, which can continuously release NGF at a local site, and could be used as a scaffold in an intravenous catheter to repair rat facial nerve defects. However, most studies have focused on loading NGF on the scaffold, and few have documented the secretion of NGF on the scaffold. In this study, more NGF was released in the three-dimensional environment, possibly owing to the increase in cell contact area. Sun et al. [48] showed that NGF could be enriched and stored in collagen. The gelatin-alginate scaffold likely promoted Schwann cell NGF secretion and storage.

Schwann cells secrete a range of neurotrophic factors, including NGF, BDNF, GDNF and PDGF, which induce axon regeneration [49–52]. The qRT-PCR results showed that, on day 4, the mRNA levels of NGF, BDNF, GDNF, and PDGF were higher in Schwann cells on the 3D bioprinted scaffold than in the 2D culture, which was consistent the ELISA results. The 3D cultured Schwann cells were likely in a more suitable environment for growth, and in better contact with each other, facilitating the secretion of NGF, BDNF, GDNF, PDGF. In addition, PDGF could promote the secretion of collagen by Schwann cells [53].

Wang et al. [54] found that 3D printed scaffolds without cells degraded after 8 weeks of implantation, leaving a small amount of irregular material. The cell-containing scaffold retained its original shape, and blood vessels grew into the pores of the construct. In this study, cell-free scaffolds were degraded after 4 weeks. The cell-containing scaffolds, although loose in structure, still showed a partial grid structure, and S-100 β immunofluorescence was positive, indicating that Schwann cells still survived in the 3D bioprinted constructs and helped to maintain scaffold shape. Gelatin without crosslink led to the insufficient strength of the bioprinted structure. Meanwhile calcium ions got displaced in an ion rich environment thus causing the breakdown of the polymer network which led to the scaffolds loose in structure [55].

In future studies, we will try to introduce methacrylamide groups into gelatin and use photocrosslinking to enhance the strength of the scaffold [56], and further verify the effect of cross-linking on cell viability and nerve scaffold function.

Studies have shown that Schwann cells and CTXOE03 cells can be directionally dispersed in collagen-containing ECM to form an engineered neural tissue construct that can potentially be used for peripheral nerve repair [57,58]. The results of this study indicated that, compared to 2D culture, the 3D bioprinted gelatin-alginate scaffold loaded with Schwann cells was more conducive to the expression of nerve regeneration-related neurotrophic factors and important nutrients by Schwann cells, which could provide potential applications for neural tissue engineering. However, our research has some shortcomings. Owing to technical limitations, the diameter of the nozzle was larger than the axon. In addition, materials were prone to degradation, volume changes, and internal morphology damage in in vivo experiments. Therefore, it is necessary to develop a material that is well suited to the 3D bioprinting of cells, and exhibits optimal resolution and sufficient strength.

5. Conclusion

In this study, a hydrogel construct with Schwann cells was successfully created by 3D bioprinting, and it was confirmed that the 3D bioprinted construct composed of gelatin and sodium alginate could maintain viability and promote adhesion of Schwann cells. The 3D construct upregulated NGF protein and mRNA expression of NGF, BDNF, GDNF, and PDGF. These preliminary results show that the 3D bioprinted gelatin-sodium alginate construct provides a suitable microenvironment for Schwann cells to maintain its activity. The 3D bioprinted gelatin-sodium alginate construct could be a promising candidate in neural tissue engineering in the future.

Declaration of competing interest

The authors declare that they have no known competing financial interests or personal relationships that could have appeared to influence the work reported in this paper.

Acknowledgments

This work was supported by National Natural Science Foundation of China (No. 81870781).

Appendix A. Supplementary data

Supplementary data to this article can be found online at <https://doi.org/10.1016/j.msec.2019.110530>.

References

- [1] R. Sullivan, T. Dailey, K. Duncan, N. Abel, C.V. Borlongan, Peripheral nerve injury: stem cell therapy and peripheral nerve transfer, *Int. J. Mol. Sci.* 17 (12) (2016).
- [2] R. Li, Z. Liu, Y. Pan, L. Chen, Z. Zhang, L. Lu, Peripheral nerve injuries treatment: a systematic review, *Cell Biochem. Biophys.* 68 (3) (2013) 449–454.
- [3] M. Asplund, M. Nilsson, A. Jacobsson, H. von Holst, Incidence of traumatic peripheral nerve injuries and amputations in Sweden between 1998 and 2006, *Neuroepidemiology* 32 (3) (2009) 217–228.
- [4] G.R.D. Evans, Peripheral nerve injury: a review and approach to tissue engineered constructs, *Anat. Rec.* 263 (4) (2001) 396–404.
- [5] C.A. Taylor, D. Braza, J.B. Rice, T. Dillingham, The incidence of peripheral nerve injury in extremity trauma, *Am. J. Phys. Med. Rehabil.* 87 (5) (2008) 381–385.
- [6] G.N. Panagopoulos, P.D. Megaloiokonomos, A.F. Mavrogenis, The present and future for peripheral nerve regeneration, *Orthopedics* 40 (1) (2017) e141–e156.
- [7] F.J. Paprottka, P. Wolf, Y. Harder, Y. Kern, P.M. Paprottka, H.-G. Machens, J.A. Lohmeyer, Sensory recovery outcome after digital nerve repair in relation to different reconstructive techniques: meta-analysis and systematic review, *Plast. Surg. Int.* 2013 (2013) 1–17.
- [8] H. Fujimaki, K. Uchida, G. Inoue, M. Miyagi, N. Nemoto, T. Saku, Y. Isobe, K. Inage, O. Matsushita, S. Yagishita, J. Sato, S. Takano, Y. Sakuma, S. Ohtori, K. Takahashi, M. Takaso, Oriented collagen tubes combined with basic fibroblast growth factor promote peripheral nerve regeneration in a 15 mm sciatic nerve defect rat model, *J. Biomed. Mater. Res. A* 105 (1) (2017) 8–14.
- [9] P. Konofaos, J. Ver Halen, Nerve repair by means of tubulization: past, present, future, *J. Reconstr. Microsurg.* 29 (3) (2013) 149–164.
- [10] S.W. Peng, C.W. Li, I.M. Chiu, G.J. Wang, Nerve guidance conduit with a hybrid structure of a PLGA microfibrillar bundle wrapped in a micro/nanostructured membrane, *Int. J. Nanomedicine* 12 (2017) 421–432.
- [11] V. Hasirci, D. Arslantunali, T. Dursun, D. Yucel, N. Hasirci, Peripheral nerve conduits: technology update, *Med. Devices Evid. Res.* 7 (2014) 405–424.
- [12] J.S. Taras, S.M. Jacoby, Repair of lacerated peripheral nerves with nerve conduits, *Tech. Hand Up. Extrem. Surg.* 12 (2) (2008) 100–106.
- [13] A.R. Dixon, S.H. Jariwala, Z. Bilis, J.R. Loverde, P.F. Pasquina, L.M. Alvarez, Bridging the gap in peripheral nerve repair with 3D printed and bioprinted conduits, *Biomaterials* 186 (2018) 44–63.
- [14] R. Ashraf, H.S. Sofi, M.A. Beigh, S. Majeed, S. Arjamand, F.A. Sheikh, Prospects of natural polymeric scaffolds in peripheral nerve tissue-regeneration, *Novel Biomaterials for Regenerative Medicine*, Springer, 2018, pp. 501–525.
- [15] Q. Li, X.X. Lei, X.F. Wang, Z.G. Cai, P.J. Lyu, G.F. Zhang, Hydroxyapatite/collagen 3D printed scaffolds and their osteogenic effects on hBMSCs, *Tissue Eng. A* 25 (2019) 1261–1271.
- [16] T. Xu, C.A. Gregory, P. Molnar, X. Cui, S. Jalota, S.B. Bhaduri, T. Boland, Viability and electrophysiology of neural cell structures generated by the inkjet printing method, *Biomaterials* 27 (19) (2006) 3580–3588.
- [17] M.D. Wang, P. Zhai, D.J. Schreyer, R.S. Zheng, X.D. Sun, F.Z. Cui, X.B. Chen, Novel crosslinked alginate/hyaluronic acid hydrogels for nerve tissue engineering, *Front. Mater. Sci.* 7 (3) (2013) 269–284.
- [18] A.M. Ferreira, P. Gentile, V. Chiono, G. Ciardelli, Collagen for bone tissue regeneration, *Acta Biomater.* 8 (9) (2012) 3191–3200.
- [19] J.A. Rowley, G. Madlambayan, D.J. Mooney, Alginate hydrogels as synthetic extracellular matrix materials, *Biomaterials* 20 (1) (1999) 45–53.
- [20] K.Y. Lee, D.J. Mooney, Alginate: properties and biomedical applications, *Prog. Polym. Sci.* 37 (1) (2012) 106–126.
- [21] S. Sakai, K. Hirose, K. Taguchi, Y. Ogushi, K. Kawakami, An injectable, in situ enzymatically gellable, gelatin derivative for drug delivery and tissue engineering, *Biomaterials* 30 (20) (2009) 3371–3377.
- [22] M. Barton, J. John, M. Clarke, A. Wright, J. Ekberg, The glia response after peripheral nerve injury: a comparison between Schwann cells and olfactory ensheathing cells and their uses for neural regenerative therapies, *Int. J. Mol. Sci.* 18 (2) (2017).
- [23] L. Ouyang, R. Yao, X. Chen, J. Na, W. Sun, 3D printing of HEK 293FT cell-laden hydrogel into macroporous constructs with high cell viability and normal biological functions, *Biofabrication* 7 (1) (2015).
- [24] Y. Zhao, R. Yao, L. Ouyang, H. Ding, T. Zhang, K. Zhang, S. Cheng, W. Sun, Three-dimensional printing of Hela cells for cervical tumor model in vitro, *Biofabrication* 6 (3) (2014).
- [25] S. England, A. Rajaram, D.J. Schreyer, X. Chen, Bioprinted fibrin-factor XIII-hyaluronate hydrogel scaffolds with encapsulated Schwann cells and their in vitro characterization for use in nerve regeneration, *Bioprinting* 5 (2017) 1–9.
- [26] C.M. Owens, F. Marga, G. Forgacs, C.M. Heesch, Biofabrication and testing of a fully cellular nerve graft, *Biofabrication* 5 (4) (2013) 045007.
- [27] H. Alizadeh Sardroud, S. Nemati, A. Baradar Khoshfetrat, M. Nabavinia, Y. Beygi Khosrowshahi, Barium-cross-linked alginate-gelatin microcapsule as a potential platform for stem cell production and modular tissue formation, *J. Microencapsul.* 34 (5) (2017) 488–497.
- [28] S. Nemati, A. Rezabakhsh, A.B. Khoshfetrat, A. Nourazarian, C. Biray Avci, B. Goker Bagca, H. Alizadeh Sardroud, M. Khaksar, M. Ahmadi, A. Delkhosh, E. Sokullu, R. Rahbarghazi, Alginate-gelatin encapsulation of human endothelial cells promoted angiogenesis in vivo and in vitro milieu, *Biotechnol. Bioeng.* 114 (12) (2017) 2920–2930.
- [29] X. Yang, Z. Lu, H. Wu, W. Li, L. Zheng, J. Zhao, Collagen-alginate as bioink for three-dimensional (3D) cell printing based cartilage tissue engineering, *Mater. Sci. Eng. C Mater. Biol. Appl.* 83 (2018) 195–201.
- [30] K.Y. Lee, D.J. Mooney, Hydrogels for tissue engineering, *J. Chem. Rev.* 101 (2001) 1869–1879.
- [31] M. Sarker, M. Izadifar, D. Schreyer, X. Chen, Influence of ionic crosslinkers (Ca²⁺)/Ba²⁺/Zn²⁺) on the mechanical and biological properties of 3D bioprinted hydrogel scaffolds, *J. Biomater. Sci. Polym. Ed.* 29 (10) (2018) 1126–1154.
- [32] B. Duan, L.A. Hockaday, K.H. Kang, J.T. Butcher, 3D bioprinting of heterogeneous aortic valve conduits with alginate/gelatin hydrogels, *J. Biomed. Mater. Res. A* 101 (5) (2013) 1255–1264.
- [33] M.D. Giuseppe, N. Law, B. Webb, A.M. R. L.J. Liew, T.B. Sercombe, R.J. Dilley, B.J. Doyle, Mechanical behaviour of alginate-gelatin hydrogels for 3D bioprinting, *J. Mech. Behav. Biomed. Mater.* 79 (2018) 150–157.
- [34] M. Hospodiu, M. Dey, D. Sosnoski, I.T. Ozbolat, The bioink: a comprehensive review on bioprintable materials, *Biotechnol. Adv.* 35 (2) (2017) 217–239.
- [35] C.H. Lubba, Y. Le Guen, S. Jarvis, N.S. Jones, S.C. Cork, A. Eftekhari, S.R. Schultz, PyPNS: multiscale simulation of a peripheral nerve in python, *Neuroinformatics* 17 (1) (2019) 63–81.
- [36] S.C. Lin, Y. Wang, D.F. Wertheim, A.G.A. Coombes, Production and in vitro evaluation of macroporous, cell-encapsulating alginate fibres for nerve repair, *Mater. Sci. Eng. C Mater. Biol. Appl.* 73 (2017) 653–664.
- [37] S. Lopes, L. Bueno, F.D. Aguiar JUNIOR, C. Finkler, Preparation and characterization of alginate and gelatin microcapsules containing *Lactobacillus rhamnosus*, *An. Acad. Bras. Cienc.* 89 (3) (2017) 1601–1613.
- [38] R. Chang, J. Nam, W. Sun, Effects of dispensing pressure and nozzle diameter on cell survival from solid freeform fabrication-based direct cell writing, *Tissue Eng. Part A* 14 (1) (2008) 41–48.
- [39] R.D. Pedde, B. Mirani, A. Navaei, T. Styan, S. Wong, M. Mehrali, A. Thakur, N.K. Mohtaram, A. Bayati, A. Dolatshahi-Pirouz, M. Nikkhab, S.M. Willerth, M. Akbari, Emerging biofabrication strategies for engineering complex tissue constructs, *Adv. Mater.* 29 (19) (2017).
- [40] L. Ouyang, R. Yao, Y. Zhao, W. Sun, Effect of bioink properties on printability and cell viability for 3D bioplotting of embryonic stem cells, *Biofabrication* 8 (3) (2016) 035020.
- [41] Y. Yu, Y. Zhang, J.A. Martin, I.T. Ozbolat, Evaluation of cell viability and functionality in vessel-like bioprintable cell-laden tubular channels, *J. Biomech. Eng.* 135 (9) (2013) 91011.
- [42] D.B. Zimmer, E.H. Cornwall, A. Landar, W. Song, The S100 protein family: history, function, and expression, *Brain Res. Bull.* 37 (4) (1995) 417–429.
- [43] J.R. Soucy, E. Shirzaei Sani, R. Portillo Lara, D. Diaz, F. Dias, A.S. Weiss, A.N. Koppes, R.A. Koppes, N. Annabi, Photocrosslinkable gelatin/tropoelastin hydrogel adhesives for peripheral nerve repair, *Tissue Eng. Part A* 24 (17–18) (2018) 1393–1405.
- [44] A.C. Lee, V.M. Yu, J.B. Lowe, M.J. Brenner, D.A. Hunter, S.E. Mackinnon, S.E. Sakiyama-Elbert, Controlled release of nerve growth factor enhances sciatic nerve regeneration, *Exp. Neurol.* 184 (1) (2003) 295–303.
- [45] J. Chen, Y.F. Chu, J.M. Chen, B.C. Li, Synergistic effects of NGF, CNTF and GDNF on functional recovery following sciatic nerve injury in rats, *Adv. Med. Sci.* 55 (1) (2010) 32–42.
- [46] R. Li, Y. Li, Y. Wu, Y. Zhao, H. Chen, Y. Yuan, K. Xu, H. Zhang, Y. Lu, J. Wang, X. Li, X. Jia, J. Xiao, Heparin-polyoxamer thermosensitive hydrogel loaded with bFGF and NGF enhances peripheral nerve regeneration in diabetic rats, *Biomaterials* 168 (2018) 24–37.
- [47] X. Chao, L. Xu, J. Li, Y. Han, X. Li, Y. Mao, H. Shang, Z. Fan, H. Wang, Facilitation of facial nerve regeneration using chitosan-beta-glycerophosphate-nerve growth factor hydrogel, *Acta Otolaryngol.* 136 (6) (2016) 585–591.
- [48] W. Sun, C. Sun, H. Lin, H. Zhao, J. Wang, H. Ma, B. Chen, Z. Xiao, J. Dai, The effect of collagen-binding NGF-β on the promotion of sciatic nerve regeneration in a rat sciatic nerve crush injury model, *Biomaterials* 30 (27) (2009) 4649–4656.
- [49] J. Qin, L. Wang, Y. Sun, X. Sun, C. Wen, M. Shahmoradi, Y. Zhou, Concentrated growth factor increases Schwann cell proliferation and neurotrophic factor secretion and promotes functional nerve recovery in vivo, *Int. J. Mol. Med.* 37 (2) (2016) 493–500.
- [50] A. Shakhbazov, J. Kawasoe, S.A. Hoyng, R. Kumar, J. van Minnen, J. Verhaagen, R. Midha, Early regenerative effects of NGF-transduced Schwann cells in peripheral nerve repair, *Mol. Cell. Neurosci.* 50 (1) (2012) 103–112.
- [51] N. Garcia, M.M. Santafe, M. Tomas, M.A. Lanuza, N. Besalduch, J. Tomas, Involvement of brain-derived neurotrophic factor (BDNF) in the functional elimination of synaptic contacts at polyinnervated neuromuscular synapses during development, *J. Neurosci. Res.* 88 (7) (2010) 1406–1419.
- [52] Y.J. Chen, J.X. Zhang, L. Shen, Q. Qi, X.X. Cheng, Z.R. Zhong, Z.Q. Jiang, R. Wang, H.Z. Lu, J.G. Hu, Schwann cells induce proliferation and migration of oligodendrocyte precursor cells through secretion of PDGF-AA and FGF-2, *J. Mol. Neurosci.* 56 (4) (2015) 999–1008.
- [53] H. Jiang, W. Qu, Y. Li, W. Zhong, W. Zhang, Platelet-derived growth factors-BB and fibroblast growth factors-base induced proliferation of Schwann cells in a 3D environment, *Neurochem. Res.* 38 (2) (2013) 346–355.
- [54] X.F. Wang, Y. Song, Y.S. Liu, Y.C. Sun, Y.G. Wang, Y. Wang, P.J. Lyu, Osteogenic differentiation of three-dimensional bioprinted constructs consisting of human adipose-derived stem cells in vitro and in vivo, *PLoS One* 11 (6) (2016).
- [55] A.G. Tabriz, M.A. Hermida, N.R. Leslie, W. Shu, Three-dimensional bioprinting of complex cell laden alginate hydrogel structures, *Biofabrication* 7 (4) (2015).
- [56] J. Tao, J. Zhang, T. Du, X. Xu, X. Deng, S. Chen, J. Liu, Y. Chen, X. Liu, M. Xiong,

- Y. Luo, H. Cheng, J. Mao, L. Cardon, M. Gou, Y. Wei, Rapid 3D printing of functional nanoparticle-enhanced conduits for effective nerve repair, *Acta Biomater.* 90 (2019) 49–59.
- [57] M. Georgiou, S.C.J. Bunting, H.A. Davies, A.J. Loughlin, J.P. Golding, J.B. Phillips, Engineered neural tissue for peripheral nerve repair, *Biomaterials* 34 (30) (2013) 7335–7343.
- [58] C. O'Rourke, A.G.E. Day, C. Murray-Dunning, L. Thanabalasundaram, J. Cowan, L. Stevanato, N. Grace, G. Cameron, R.A.L. Drake, J. Sinden, J.B. Phillips, An allogeneic 'off the shelf' therapeutic strategy for peripheral nerve tissue engineering using clinical grade human neural stem cells, *Sci. Rep.* 8 (1) (2018) 2951.